Indentation of an Oriented Transparent Polyamide

Y. Yang,[1] G. Thompson,[2] J. Song,[3] A. Hiltner,[1] E. Baer[1]

[1]*Center for Applied Polymer Research, Macromolecular Science and Engineering Department, Case Western Reserve University, Cleveland, OH 44106-7202*
[2]*U.S. Army Dental and Trauma Research Detachment, 310B B Street, Building 1H, Great Lakes, IL 60088-5259*
[3]*U.S. Army Natick Soldier Research, Development and Engineering Center, AMSRD-NSR-WS-DB, Natick, MA 01760-5000*

Received 13 May 2008; accepted 23 August 2008
DOI 10.1002/app.29350
Published online 22 December 2008 in Wiley InterScience (www.interscience.wiley.com).

ABSTRACT: In this study, the effect of orientation on the indentation hardness and energy absorption of an oriented transparent Trogamid polyamide was investigated with a spherical indentation methodology. It was found that the orientation significantly improved the indentation hardness and energy absorbed by plastic deformation. From the indentation hardness measurement, the elastic modulus, yield stress, and strain hardening exponent were derived from both the elastic and plastic regions of the indentation load–displacement curves. The elastic modulus was found to remain the same with orientation; the yield stress and the strain hardening exponent increased with orientation. The increase in the strain hardening exponent was the primary reason for the improved indentation hardness and energy absorption in the oriented samples. The mechanical properties from indentation measurements were compared to values obtained from tension true stress/true strain measurements. Good agreement was observed between the results from the indentation and tension tests. The effect of temperature on the mechanical properties was also studied. It was found that the modulus and yield stress were higher at a lower temperature; however, the strain hardening exponent remained unaffected. © 2008 Wiley Periodicals, Inc. J Appl Polym Sci 112: 163–172, 2009

Key words: hardness; indentation; orientation; polyamides; toughness

INTRODUCTION

Hardness is an important mechanical property of materials. It is the measurement of material resistance to local deformation. Materials with higher hardness have better resistance to denting, scratching, and abrasion.[1] Indentation experiments have long been used to measure the hardness of materials, including metals, ceramics, and polymers.[2–4] In indentation hardness measurement, the indenter is forced into the surface of the test material and then released. Three important quantities are measured from the loading–unloading test cycle: the peak load, the maximum displacement, and the elastic recovery. The peak load normalized to the projected area of impression is then the hardness of the material.

Surface contacts between the indenter and test materials are highly dependent on their respective mechanical properties. In addition to material hardness, various investigators have tried to extract other mechanical properties from indentation hardness measurements. Relations between uniaxial tension and indentation tests were initially directed toward the measurement of the plastic properties of metals.[3] Oliver and Pharr[5] introduced a method for measuring the elastic modulus from the unloading part of the load–displacement curve or the unloading stiffness. Comparisons between uniaxial tension and indentation tests on polymers were initially reported by Baer et al.[4] Balta Calleja et al.[6] widely investigated the correlation of the microhardness with the morphology and microstructure of polymers. The measurement of mechanical parameters by indentation experiments has made considerable progress in recent years, and it is now used to measure mechanical properties such as the elastic modulus, yield stress, and strain hardening exponent.[7–13]

Recent research on indentation has been generally conducted with a microindenter or nanoindenter because they can make highly localized measurements with a small amount of a sample. However, inelastic deformation of the specimen may be induced at very small loads, so the analysis is usually done with the unloading curve. For the determination of the elastic modulus from the unloading curve, the radius of curvature of the contact area needs to be determined, and the following difficulties might be faced: (1) microscopic tips of the indenter may not be perfectly spherical, so their effective diameter changes with the depth of indentation, and (2) the material around an indenter may pile up or sink in with respect to the original surface of the specimen because of permanent inelastic

Correspondence to: A. Hiltner (pah6@case.edu).

deformation. Hence, the determination of the maximum contact area is difficult. Also, for specimens that are not uniform and have surface roughness, such as polycrystalline materials, blends, and materials with fillers, the obtained properties may not represent the bulk properties. By the measurement of the hardness with a macroindenter, these disadvantages can be overcome, and bulk properties of a material can be reliably related to its hardness.

Orientation has been known to improve the mechanical properties of materials.[14] Previous studies have shown that the tension yield stress, fracture strength, and puncture resistance of polypropylene are increased by biaxial orientation.[15–17] Polyamide has been widely used for engineering components because of its excellent mechanical properties. A study has shown that the mechanical properties, including the modulus and tensile strength, can be further improved by orientation.[18] However, to date, the effect of orientation on the indentation hardness of polyamide has not been investigated. Using a spherical macroindentation methodology, this work elucidates the effect of orientation on the indentation hardness and energy absorption of a transparent polyamide. From the indentation hardness measurement, the elastic modulus, yield stress, and strain hardening exponent were determined, and the effects of orientation on the hardness and energy absorption were elucidated. To understand the elastic and plastic properties from indentation experiments, a detailed comparison with the mechanical properties in tension was conducted.

EXPERIMENTAL

All specimens used in this investigation were prepared from injection-molded sheets of CX7323-grade Trogamid polyamide (Degussa AG, Duesseldorf, Germany). The sheets had dimensions of 153 mm × 153 mm (6″ × 6″). The initial thicknesses of the samples varied from 3.2 to 12.8 mm, so the final thickness after cross-rolling was about 3.2 mm. Before indentation and tension testing, the Trogamid specimens were oriented by solid-phase cross-rolling. The instrument for cross-rolling has been described in a previous study.[15] Before rolling, each sample was heated to 100°C in an oven for 30 min. The sample was then pushed through the gap between the two small rolls, which was 0.127 mm smaller than the original thickness of the Trogamid sheet. When the Trogamid sheet passed through the rolls, it was compressively oriented. This procedure was repeated many times; each time, the gap was decreased by 0.127 mm, and the Trogamid sheet was flipped over and rotated 90° for each successive pass. In this way, the thickness of the Trogamid sheet was reduced, and biaxial orientation was achieved. Three oriented samples with 50, 67, and 75% thickness reduction were made for this study, and they are called CX7323 (50%), CX7323 (67%), and CX7323 (75%), respectively, in the future discussion. All three samples had a final sheet thickness of 3.2 mm after cross-rolling. Samples with 50% thickness reduction had an equal biaxial orientation ratio of 1.4 × 1.4, samples with 67% thickness reduction had an equal biaxial orientation ratio of 1.7 × 1.7, and samples with 75% thickness reduction had an equal biaxial orientation ratio of 2.0 × 2.0. An unoriented sample with the same thickness (3.2 mm) was used as the control for this study.

Orientation in the cross-rolled Trogamid sheets was characterized with the birefringence. The measurements were made with a Metricon (Pennington, NJ) model 2010 prism coupler using a 633-nm wavelength laser. The refractive indices along three mutually perpendicular axes (n_x, n_y, and n_z) were measured to calculate the birefringence.

The indentation hardness measurements were performed with an Instron model 8500 hydraulic system. A steel spherical indenter with a tip diameter of 9 mm was used for this study. The test samples were cut to a length of 50.8 mm and a width of 25.4 mm with a bandsaw. The edges were flattened by polishing with 1200-grit sandpaper. Test samples were placed on a flat metal support, and the indentation tests were done at the ambient temperature with a crosshead speed of 10 mm/min.

A schematic of the two-loading indentation procedure is shown in Figure 1. It was used to determine the elastic work and plastic work during indentation deformation. First, a load was applied onto the sample, and this resulted in both elastic and plastic deformation because the deformation from the reapplied load was the same as the recovered deformation from the first loading. When the load was removed, the elastic deformation in the sample was then allowed to recover for 10 min, and only the irreversible plastic deformation remained. Subsequently, the same amount of load was reapplied to the sample, and this resulted in only elastic deformation. A typical load–displacement curve for this type of two-loading indentation measurement is shown in Figure 2. From the first loading, the total work of indentation deformation (W_t) was determined as the area below the first loading curve. The elastic work of indentation deformation (W_e) was determined as the area below the second loading curve. The plastic work (W_p) was calculated by subtraction of the elastic work from the total work ($W_p = W_t - W_e$).

After release of the load, the elastic deformation was recovered, and only the plastic deformation remained as permanent residual deformation.[19,20] The diameter ($2a$) of the residual deformation, a spherical cap, was measured with an Olympus (Center Valley, PA) BH-2 optical microscope after the

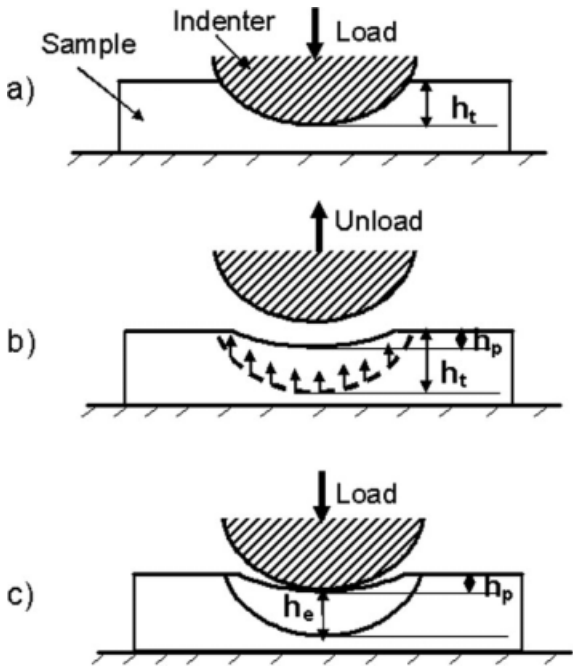

Figure 1 Schematic showing the two-loading indentation procedure: (a) first loading, (b) elastic recovery, and (c) second loading.

sample was allowed to recover for 24 h under ambient conditions. The sample was then cut along the center of the permanently deformed area and polished. The height (h_p) of the spherical cap was measured with the optical microscope.

The uniaxial tension experiments were performed with an MTS (Eden Prairie, MN) Alliance RT30 with ASTM D 1708 test specimens with dimensions of 50 × 6.5 × 3.2 mm^3 (length × width × thickness) at a strain rate of 1%/min. For the determination of the true stress/true strain, a pattern was coated on specimens by the deposition of 200 Å of gold over a square grid with 30 wires per inch.[21] An Olympus C-5050ZOOM digital camera was used to photograph the specimen deformation every 20 s. The true strain and true stress were then analyzed.

Low-temperature indentation and tension testing was conducted at −40°C to study the effect of temperature on the elastic and plastic properties. The testing was done with a liquid-nitrogen-cooled environment chamber. After the temperature had reached the set point, the chamber was equilibrated for 15 min before the testing was started.

RESULTS AND DISCUSSION

Characterization of orientation in cross-rolled Trogamid sheets

The orientation of Trogamid sheets was characterized with birefringence measurements. The refractive indices along three mutually perpendicular axes

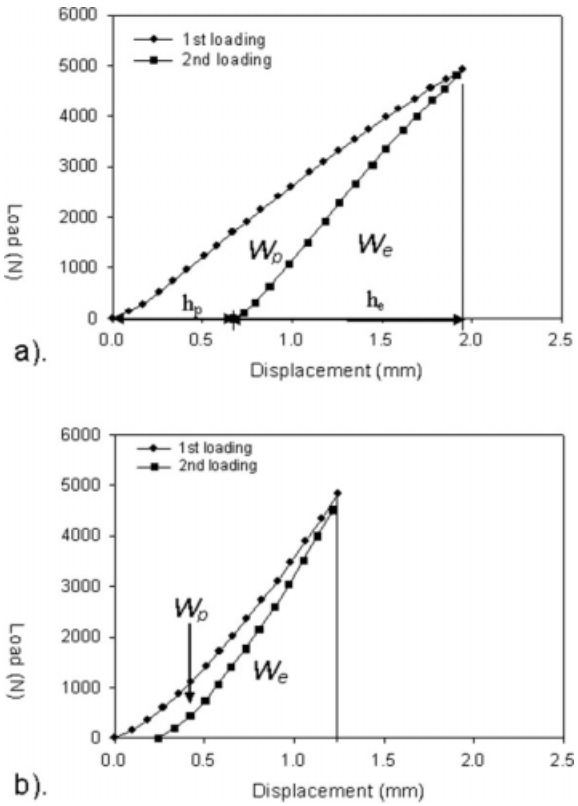

Figure 2 Determination of the elastic work (W_e) and plastic work (W_p) from the indentation first and second loadings: (a) CX7323 control and (b) CX7323 (75%).

(n_x, n_y, and n_z) were measured, and the birefringence was calculated with the following expression[22]:

$$\Delta n = \frac{n_x + n_y}{2} - n_z \quad (1)$$

where Δn is the birefringence, n_x and n_y are the refractive indices measured in the plane of the sheet, and n_z is the refractive index through the thickness of the sheet.

Figure 3 shows the effect of cross-rolling thickness reduction on the birefringence of Trogamid sheets.

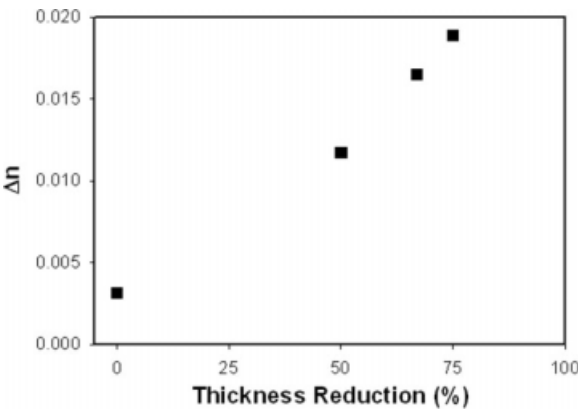

Figure 3 Effect of cross-rolling thickness reduction on sample birefringence (Δn).

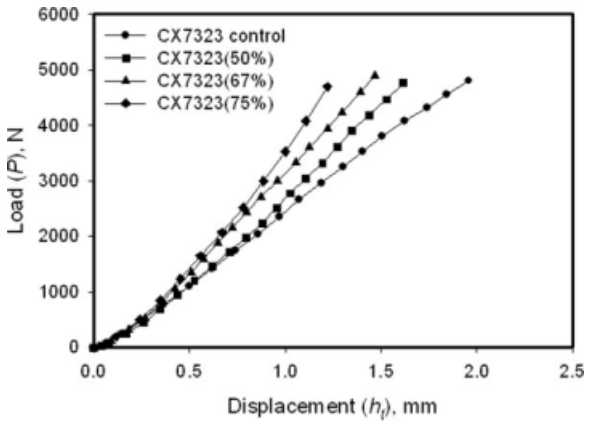

Figure 4 Effect of orientation on the indentation load–displacement curve at RT.

An increase in thickness reduction by cross-rolling resulted in an increase in birefringence, which indicated an increase in the degree of orientation. The in-plane refractive indices n_x and n_y differed by less than 10%, indicating that the samples were essentially equally biaxially oriented in the x and y directions. Because Trogamid sheets are transparent and contain very low crystallinity, the increase in birefringence with orientation is mainly due to amorphous chain orientation.

Effect of orientation on the indentation hardness of cross-rolled Trogamid sheets

Figure 4 shows the effect of orientation on the load–displacement curves of Trogamid. As expected, the load–displacement curves show two regions. The first region, which is the elastic region, is observed at smaller loads. For this region, the load–displacement relation can be described by the well-known Hertz elastic contact theory. It was found that orientation had virtually no effect on the load–displacement curves in the elastic region. With the load increasing beyond the elastic limit, yielding occurred, and irreversible plastic deformation could be observed. In this region, orientation showed a large effect on the load–displacement curves. At the load of 5000 N, the displacement decreased significantly with increasing orientation. The ball hardness under load was calculated for the oriented Trogamid sheets with the following equation:

$$H = \frac{P}{\pi D h_t} \tag{2}$$

where H is the ball hardness under load, P is the load, D is the diameter of the indenter, and h_t is the displacement. The results are shown in Table I. The ball hardness under load increased with orientation. Compared to the unoriented control, the 75% cross-rolled sample showed an increase of about 60% in ball hardness.

The ball hardness under load includes contributions from both the elastic deformation and plastic deformation. The elastic deformation recovered after removal of the load, and only the plastic deformation remained as permanent deformation. Optical microscopy images of the plastic deformation of the Trogamid sheets are shown in Figure 5(a–d). It was found that the diameter of the plastic deformation was smaller than the *in situ* contact diameter calculated from the displacement of the indenter.[23] To establish the resistance to permanent deformation, the plastic hardness (H_{plastic}) should be used, which is defined as the peak load (P) over the projected permanent deformed area (A_{proj}):

$$H_{\text{plastic}} = P/A_{\text{proj}} \tag{3}$$

The projected permanent plastic area was calculated from $A_{\text{proj}} = \pi D^2/4$, where D is the diameter of the plastic deformation. Table I shows the effect of orientation on the plastic hardness of Trogamid sheets. The results show that the plastic hardness increased significantly with increasing orientation, and the plastic hardness of the 75% cross-rolled sample increased by as much as 50% in comparison with the unoriented control.

Effect of orientation on the indentation energy absorption of cross-rolled Trogamid sheets

In the indentation tests, there are two components to energy absorption: the elastic work and the plastic work. The resistance to permanent deformation can

TABLE I
Mechanical Properties of Cross-Rolled Trogamid Determined from Indentation and Tension Tests

Designation	Thickness reduction (%)	Ball hardness (MPa)	Plastic hardness (MPa)	Yield stress (MPa)		Elastic modulus (MPa)		Strain hardening exponent	
				Indentation	Tension	Indentation	Tension	Indentation	Tension
CX7323 control	—	87	144	48	48	1280	1200	0.04	0
CX7323 (50%)	50	104	189	63	55	1240	1250	0.28	0.27
CX7323 (67%)	67	118	198	66	65	1220	1220	0.44	0.40
CX7323 (75%)	75	136	213	71	70	1210	1190	0.56	0.56

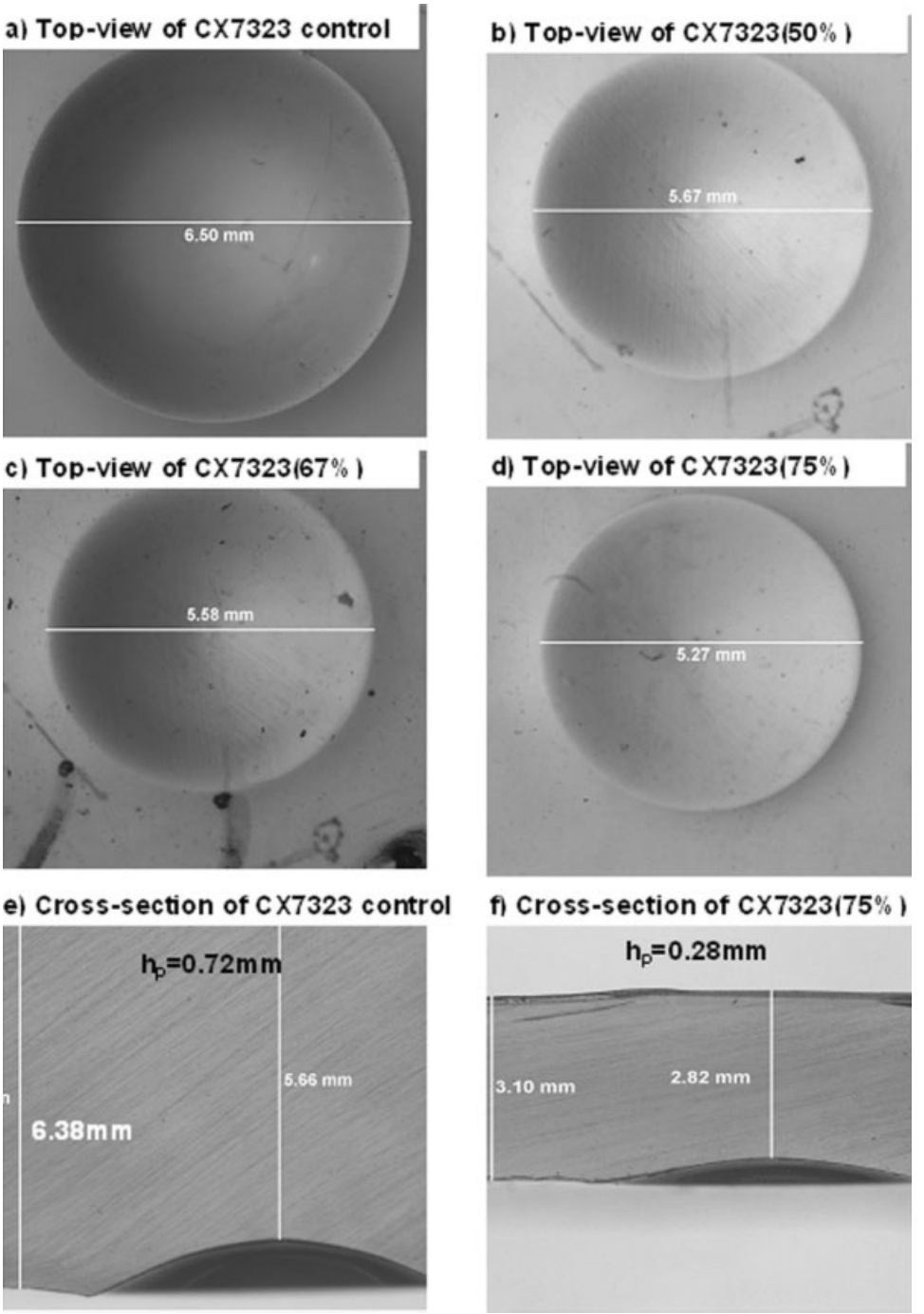

Figure 5 Optical micrographs showing the effect of orientation on indentation plastic deformation at RT under a load of 5000 N: (a) top view of the CX7323 control, (b) top view of CX7323 (50%), (c) top view of CX7323 (67%), (d) top view of CX7323 (75%), (e) cross-section view of the CX7323 control, and (f) cross-section view of CX7323 (75%).

also be assessed by the plastic work divided by the volume of the plastic deformation.[24] The total work is the area under the first indentation curve. The elastic work is given by the area under the second loading curve. The plastic work is the difference between the total work and the elastic work.

Figure 2 shows the determination of the elastic work and the plastic work for the control and oriented CX7323 (75%). The elastic work and plastic work at all other levels of loading are listed in Table II. It was found that the elastic work was higher than the plastic work for all the loading conditions.

The volume of the plastic deformation is obtained from the measured diameter ($2a$) and the height (h_p) of the plastic deformation. Figure 5(a,e) shows the optical microscopy images of the diameter and height of the plastic deformation of the unoriented control, respectively; Figure 5(d,f) shows the

TABLE II
Effect of Orientation on the Plastic Work and Plastic Volume

	CX7323 control			CX7323 (75%)		
Load (N)	Elastic work (J)	Plastic work (J)	Plastic volume (mm^3)	Elastic work (J)	Plastic work (J)	Plastic volume (mm^3)
1000	0.18	0	0	0.17	0	0
2000	0.48	0.10	0.8	0.46	0.09	0.5
3000	1.05	0.35	2.7	0.94	0.20	1.0
4000	2.10	0.77	7.0	1.33	0.42	1.9
5000	2.96	1.42	12.1	1.88	0.65	3.1

diameter and height of the plastic deformation of CX7323 (75%), respectively. At the same load, both the diameter and the height of the plastic deformation for CX7323 (75%) were smaller than those of the unoriented control. The plastically deformed volume (V_p) was calculated with the following equation

$$V_p = (\pi/6)\left(3a^2 + h_p^2\right)h_p \tag{4}$$

The plastic volumes of CX7323 (75%) and the control at different loading levels are given in Table II. The results show that the plastic volume increased with the load for both the control and CX7323 (75%). However, at the same level of loading, the plastic volume of the control was much larger than that of the oriented sample. At the load of 5000 N, the plastic volume of the control was almost 4 times that of the 75% cross-rolled sample.

Figure 6 shows a plot of the work absorbed by plastic deformation against the plastic volume for both the control and oriented CX7323 (75%). It was found that the plastic work increased linearly with the plastic volume for both CX7323 (75%) and the control. However, at the same plastic volume, the plastic work absorbed by the 75% cross-rolled sample was greater than that absorbed by the unoriented control.

Effect of orientation on the mechanical behavior with indentation measurements

Elastic modulus

The elastic modulus can be calculated from the elastic regime of the load–displacement curve (Fig. 4) by the well-known Hertz elastic contact theory[25,26]:

$$P = \frac{4E^*\sqrt{R}}{3}h_t^{3/2} \tag{5}$$

where P is the load, h_t is the displacement, R is the radius of the indenter, and E^* is the composite elastic modulus of the particular specimen–indenter system. When the elastic modulus of the metal indenter is much greater than the specimen, E^* can be calculated as follows[12]:

$$E^* = \frac{E}{1-\nu^2} \tag{6}$$

where E is the elastic modulus of the specimen and ν is Poisson's ratio of the specimen. By the combination of eq. (5) and (6), the elastic modulus of the specimen can then be calculated with the following equation:

$$E = \frac{3(1-\nu^2)P}{4\sqrt{R}h_t^{3/2}} \tag{7}$$

The elastic modulus determined from the elastic region is shown in Table I. The results show that the elastic modulus did not change with orientation, and this was probably because the polymer chain orientation was not high enough to affect the elastic modulus.

Yield stress

When a relatively large load is applied in the indentation test, the material beneath the indenter is permanently deformed. Under that condition, the mean pressure is 3 times the yield stress for a spherical

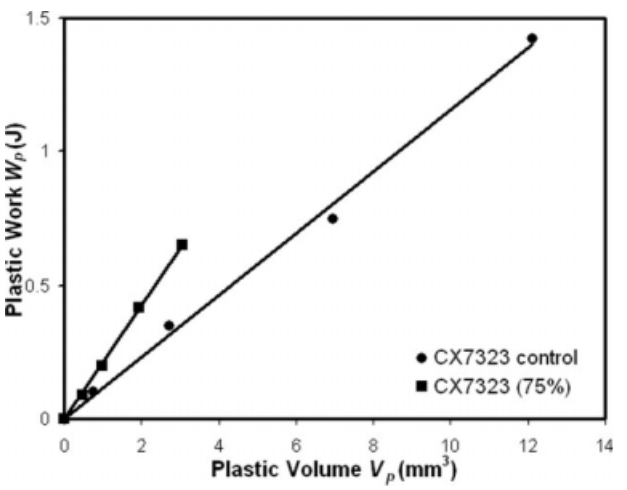

Figure 6 Comparison of the plastic work as a function of the plastic volume for the unoriented control and 75% cross-rolled sample.

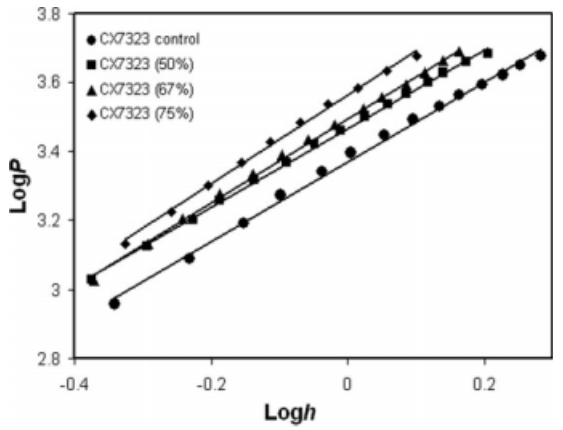

Figure 7 Effect of orientation on the strain hardening exponent as determined from the plastic region of indentation load–displacement curves.

indentation, and it follows that the yield stress of a material can be calculated from indentation hardness measurements.[13,27] Tabor[28] conclusively showed that the plastic hardness is 3 times the yield stress:

$$H_{\text{plastic}} = P/A_{\text{proj}} = 3\sigma_y \tag{8}$$

where σ_y is the yield stress. The projected permanent plastic area was calculated as discussed before. From eq. (8), the yield stresses were determined for the oriented samples and the control. The results are given in Table I. These results showed that the yield stress increases with increasing orientation. The yield stress of CX7323 (75%) increased by as much as 50% versus that of the control.

Knowing the yield stress, we can calculate the critical load at the yielding point according to Von Mises's yielding criteria. According to Johnson,[25] the first yield for a spherical indentation occurs at

$$P_m = 1.1\sigma_y \tag{9}$$

where P_m is the mean pressure. Using this correlation gives a critical load at yielding of about 200 N for the unoriented control and about 700 N for CX7323 (75%). This confirms that for an indentation with a load of 5000 N, the majority of the load–displacement curve is in the plastic region.

Strain hardening

The strain hardening exponent can be determined from the fully plastic region of the load–displacement curve. Alcala et al.[12] showed that in the fully plastic regime, the relationship between the load and the indentation displacement can be described as follows:

$$P \propto h^{1+n/2} \tag{10}$$

where n is the strain hardening exponent, P is the load, and h is the indentation displacement. By plotting log P against log h, we calculated the strain hardening exponent from the slope of the linear fit. As shown in Figure 7, log P versus log h plots for both the oriented and control materials were linear. It was found that the strain hardening exponent increased with increasing orientation. Because the majority of the energy absorption was in the strain hardening region, the higher strain hardening exponent was primarily responsible for the increasing energy absorption with orientation.

Determination of the mechanical properties from uniaxial tension testing

Figure 8 shows the effect of orientation on the true stress (σ)/true strain (ε) behavior from uniaxial tension measurements. The σ–ε curve can be divided into two regions: the elastic region for $\sigma \leq \sigma_y$ and the plastic region for $\sigma > \sigma_y$. For the elastic region, the σ–ε relationship can be described by the linear model: $\sigma = E\varepsilon$. For the plastic region, the relationship of σ and ε can be described by the power-law model: $\sigma = K\varepsilon^n$, where K is a material constant.[9,10] The elastic modulus and the yield stress were obtained from the stress–strain curve and are given in Table I. As with indentation, the elastic modulus did not change with orientation, and the yield stress increased with increasing orientation. The strain hardening exponent was determined through the plotting of log σ against log ε for the plastic region of the σ–ε curve and is shown in Figure 9. From the linear fit of log σ against log ε, the strain hardening exponent for all samples was obtained. The results are given in Table I. It was found that the strain hardening exponent increased significantly with orientation.

The elastic and plastic properties measured by indentation were compared with the values obtained from tension experiments. The elastic modulus, the yield stress, and the strain hardening exponent from

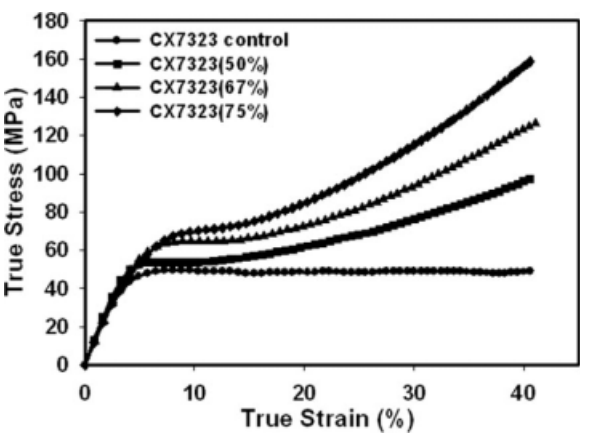

Figure 8 Effect of orientation on the uniaxial true stress/true strain curve of cross-rolled Trogamid sheets at RT.

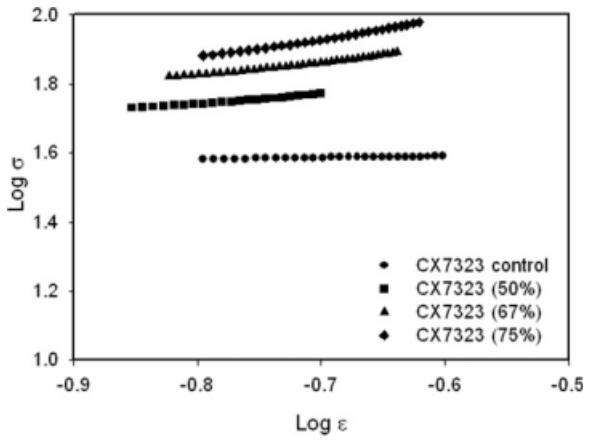

Figure 9 Effect of orientation on the strain hardening exponent as determined from the plastic region of tension stress–strain curves.

indentation measurements were found to be in good agreement with the values obtained from tension measurements.

Effect of temperature on the indentation and tension properties of cross-rolled Trogamid sheets

Load–displacement curves for indentation testing at −40°C are shown in Figure 10. At a load of 7000 N, the displacement for CX7323 (75%) was about 35% smaller than that of the control. This shows that the hardness of CX7323 (75%) increased by about 35% in comparison with that of the control. The moduli calculated from the elastic regime of the curves are shown in Table III. Like the results at room temperature (RT), the modulus did not change with orientation at −40°C. The optical micrographs of the plastic deformation are shown in Figure 11. At the load of 7000 N, the plastic area of the CX7323 control was about 50% larger than that of CX7323 (75%). The value of the yield stress calculated from the plastic

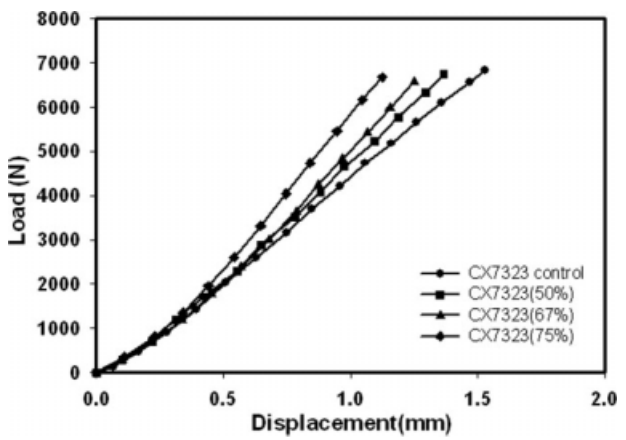

Figure 10 Effect of orientation on the indentation load–displacement curve at −40°C.

TABLE III
Effect of Temperature on the Mechanical Properties as Determined from Indentation Tests

	Modulus (MPa)		Yield stress (MPa)		Strain hardening exponent	
Sample	RT	−40°C	RT	−40°C	RT	−40°C
CX7323 control	1280	1740	48	90	0.04	0.04
CX7323 (50%)	1240	1770	63	108	0.28	0.28
CX7323 (67%)	1220	1770	66	117	0.44	0.48
CX7323 (75%)	1210	1800	71	133	0.56	0.56

hardness was about 50% higher for the 75% cross-rolled sample than for the control (Table III). As expected, the strain hardening exponent at −40°C, determined from the linear fit of log P against log h in the plastic region, also increased with orientation. The true stress–strain curve for tension testing at −40°C is shown in Figure 12, and as in the case of RT measurement, the mechanical properties obtained from tension tests at −40°C closely matched the results from the indentation tests at −40°C.

The mechanical properties from indentation measurements at RT are compared with those at −40°C in Table III. At −40°C, the modulus increased about 40%. This increase was much smaller than that of polypropylene, which increased by almost a factor of 3.[15] The smaller increase in the modulus is consistent with dynamic mechanical thermal analysis measurement in literature.[29] As expected, the yield stress at −40°C also increased in comparison with that at RT. The yield stress at −40°C showed an increase of about 70% in comparison with that at RT. Surprisingly, the temperature showed almost no effect on the strain hardening exponent in this oriented polymer. Previously reported results for unoriented polycarbonate showed that the strain hardening coefficient increased with decreasing temperature.[30]

CONCLUSIONS

The effect of orientation on the mechanical properties of Trogamid polyamide was investigated with spherical indentation measurements. Cross-rolling induced orientation in Trogamid polyamide sheets, and with increasing thickness reduction in cross-rolling, the amount of orientation increased. The hardness and energy absorption of Trogamid polyamide sheets increased with orientation. With 75% thickness reduction, the hardness of Trogamid increased by as much as 60% versus that of the unoriented sheet. For the same amount of plastic deformation, the energy absorbed by the 75% cross-rolled sample almost doubled in comparison with that of the

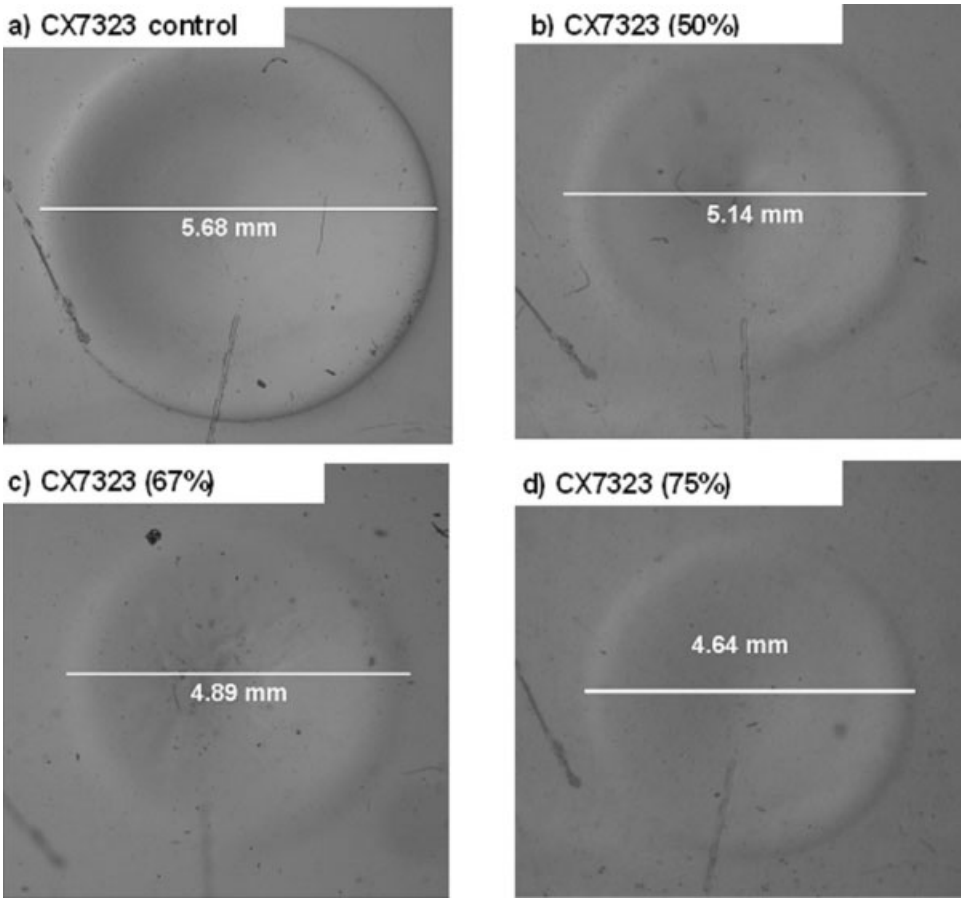

Figure 11 Effect of orientation on the permanent plastic deformation at −40°C under an indentation load of 7000 N.

unoriented sheet. The elastic modulus, yield stress, and strain hardening exponent were determined from the indentation hardness measurements and compared to those determined from uniaxial tension tests. Good agreement between the results of the two methodologies was found. The orientation increased the yield stress and strain hardening exponent. The increasing strain hardening exponent with orientation was primarily responsible for the higher hardness and energy absorption in the oriented samples. The modulus and yield stress increased with decreasing temperature; however, the strain hardening exponent was not affected by temperature.

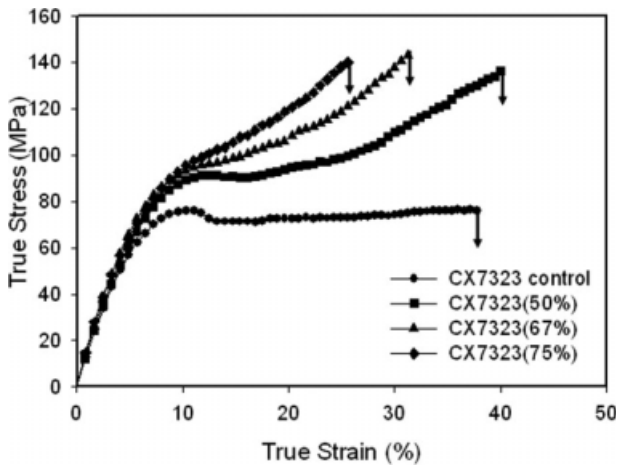

Figure 12 Effect of orientation on the uniaxial tension true stress/true strain curve of cross-rolled Trogamid sheets at −40°C.

References

1. Balta Calleja, F. J.; Fakirov, S. Microhardness of Polymers; Cambridge University Press: Cambridge, England, 2000.
2. Yu, W.; Blanchard, J. J Mater Res 1996, 11, 2358.
3. O'Neill, H. Hardness Measurements of Metals and Alloys; Chapman & Hall: New York, 1967.
4. Baer, E.; Maier, R.; Peterson, R. Soc Plast Eng J 1961, 1203.
5. Oliver, W.; Pharr, G. J Mater Res 1992, 7, 1564.
6. Balta Calleja, F.; Privalko, E.; Fainleib, A.; Shantalii, T.; Privalko, V. J Macromol Sci Phys 2000, 39, 131.
7. VanLandingham, M. J Res Natl Inst Stand Technol 2003, 108, 249.
8. Oliver, W.; Pharr, G. J Mater Res 2004, 19, 3.
9. Dao, M.; Chollacoop, N.; Van Vliet, K. J.; Venkatesh, T. A.; Suresh, S. Acta Mater 2001, 49, 3899.
10. Chollacoop, N.; Dao, M.; Suresh, S. Acta Mater 2003, 51, 3713.

11. Bucaille, J.; Stauss, S.; Felder, E.; Michler, J. Acta Mater 2003, 51, 1663.
12. Alcala, J.; Giannakopoulos, A.; Suresh, S. J Mater Res 1998, 13, 1390.
13. Neideck, K.; Franzel, W.; Grau, P. J Macromol Sci Phys 1999, 38, 669.
14. Ward, I. Structure and Properties of Oriented Polymers; Chapman & Hall: New York, 1997.
15. Snyder, J.; Hiltner, A.; Baer, E. J Appl Polym Sci 1994, 52, 217.
16. Bartczak, Z.; Morawiec, J.; Galeski, A. J Appl Polym Sci 2002, 86, 1413.
17. Yang, Y.; Thompson, G.; Hiltner, A.; Baer, E. Soc Plast Eng Annu Tech Conf Proc 2006, p 2027.
18. Ajji, A.; Legros, N.; Dumoulin, M. Adv Perform Mater 1998, 5, 117.
19. Kent, R. J Phys D 1981, 14, 601.
20. Tweedie, C.; Vliet, K. J Mater Res 2006, 21, 3029.
21. Bensason, S.; Stepanov, E.; Chum, S.; Hiltner, A.; Baer, E. Macromolecules 1997, 30, 2436.
22. Taraiya, K.; Orchard, G.; Ward, I. J Appl Polym Sci 1990, 41, 1659.
23. Kent, R. J. J Phys D 1981, 14, 601.
24. Beegan, D.; Chowdhury, S.; Laugier, M. Surf Coat Technol 2005, 192, 57.
25. Johnson, K. L. Contact Mechanics; Cambridge University Press: Oxford, 1987.
26. Timoshenko, S.; Goodier, J. Theory of Elasticity; McGraw-Hill: New York, 1951.
27. Balta Calleja, F. J.; Cagiao, M. E.; Adhikari, R.; Michler, G. H. Polymer 2004, 45, 247.
28. Tabor, D. The Hardness of Metals; Clarendon: Oxford, 1951.
29. Song, J.; Lofgren, J.; Hart, K.; Tsantinis, N.; Paulson, R.; Hatfield, J. Soc Plast Eng Annu Tech Conf Proc 2006, p 2052.
30. Govaert, L.; Tervoort, T. J Polym Sci Part B: Polym Phys 2004, 42, 2041.